Methotrexate-Polymer Nanocomposites for Targeted Pulmonary Drug Delivery

Aseel Khaled Mohammad AL-Sarayrah[1], Samer Hasan Hussein-Al-Ali[1,2*], Mike Khalil Haddad[3], and Dalia Kalil[4]

[1]*Department of Basic Pharmaceutical Sciences, Faculty of Pharmacy, Isra University, Amman 11622, Jordan*

[2]*Department of Chemistry, Faculty of Sciences, Isra University, Amman 11622, Jordan*

[3]*Department of Renewable Energy Engineering, Faculty of Engineering, Isra University, Amman 11622, Jordan*

[4]*Department of Physiotherapy, Faculty of Allied Medical Sciences, Isra University, Amman 11622, Jordan*

* ***Corresponding author:***

email: samer.alali@iu.edu.jo

Received: August 30, 2023
Accepted: November 13, 2023

DOI: 10.22146/ijc.88495

Abstract: *Nanocomposite formulation is a suitable technology that enables the development of successful dry powder inhalers. The methotrexate (MTX) and polyamide-disulfide (polymer) were used as a model to form MTX-polymer nanocomposites. Different amounts of the independent variable, MTX (0.025 and 0.050 g), polymer (0.05 and 0.01 g), pH (6.7 and 11.3), and across-linker ferric chloride ($FeCl_3$) (0.05 and 0.10 g) were used. The loading efficiency and particle size were dependent variables. The optimized formula can be obtained with the highest loading efficiency and optimum particle size. This formula can be collected by using 0.025 g of drug, 0.079 g of polymer, 0.050 g of $FeCl_3$, and pH = 6.7. The release of MTX from the nanocomposites occurs in two release steps; the first release step starts from the beginning up to 60 min, followed by a continuous release phase within 60 min. The results of the NGI analysis demonstrated that 28.1% of the nominated dose in each puff reached the lower parts of the respiratory system, an indication that the nanocomposites can be used in the delivery of MTX as a respiratory system.*

Keywords: *pulmonary drug delivery; methotrexate; nanocomposites*

■ INTRODUCTION

Asthma is a chronic airway inflammatory disorder. Many cells and biological elements are involved, namely mast cells, eosinophils, T-lymphocytes, macrophages, neutrophils, and epithelial cells, which are characterized by hyper-responsive airways, difficulty breathing, and coughing [1-2]. There is now a sharp increase in global mortality and morbidity, particularly in children. Moreover, asthma therapy maintenance is very poor, with less than half of patients taking their inhaled steroids regularly, either because they need more than one dose per day or because they don't like using nebulizers multiple times because they are difficult, especially for the elderly [3-4]. As a result, there is a need to investigate a pulmonary drug delivery (PDD) model of drug binding with nanoparticles to overcome the issues of conventional drugs and improve the efficacy of asthmatic drugs [5-6].

Several studies have concluded that PDD is the most effective method for delivering systemic drugs. This is owing to the huge surface area, high vascularization, thin blood-alveolar barrier, and avoidance of first-pass metabolism in the intestine and liver. As a result, it may have higher bioavailability than orally administered medications. Furthermore, it is non-invasive, self-administered, has a rapid onset of action, does not waste medicine in the digestive system, and has fewer systemic side effects than oral parenteral therapy [7].

Pressurized metered-dose inhalers (pMDIs), a propellant, dry powder inhalers (DPIs) as non-aqueous inhalers, and nebulizers are used to deliver drugs to alveoli. The drug's particle size must fall within a certain range to deliver micronized drug particles in an aerosolized form to these devices. It is confirmed that

sufficient medication concentration is delivered to the targeted locations within the respiratory system to achieve the intended therapeutic effect if the drug droplet/particle size is appropriate for lung deposition [8-10]. When compared to pMDI, dry powder formulations have better physiological and chemical stability, are propellant-free, are simple to operate and use, require minimal patient coordination, and hence offer added value when compared to pMDI [11].

Polymeric nanoparticles (PNPs) can be characterized as synthetic or natural. Synthetic polymers have a number of unique qualities, including increasing biological availability and improving medication pharmacokinetics. Several polymers, including chitosan [12], polyethylene glycol [13], and poly(lactic-*co*-glycolic acid) [14], have been investigated for their inherent features such as low immunogenicity, biodegradability, and biocompatibility.

Methotrexate (MTX) with a formula of $C_{20}H_{22}N_8O_5$, is an analog of folic acid with an appearance of a yellow to orange-brown crystalline powder. The main target for MTX was the enzyme dihydrofolate reductase (DHFR). This enzyme is responsible for the reduction of dihydrofolate (FH2) to tetrahydrofolate (FH4). MTX has a structure similar to FH2, so it is competitively bound with DHFR, so the FH4 was not produced, and this affects DNA and RNA synthesis [15-16]. MTX is used to treat a variety of illnesses, including cancer, autoimmune disease, ectopic pregnancy, and asthma [10,17-18]. Low doses suppress neutrophil chemotaxis, which has anti-inflammatory benefits [19]. Because oral corticosteroids have so many side effects, various trials have looked into using MTX as an oral corticosteroid-sparing treatment in severe asthma. MTX appears to be an effective oral corticosteroid-sparing medication, according to studies [19-20]. There are many problems related to MTX, such as short half-life, toxic side effects, and poor water solubility. However, in the dynamic field of drug development, it is important to stay continuously at the forefront of drug development. Therefore, we studied MTX with polymer as a model drug. The goal of this study is to create dry powder inhalers that are administered directly to the lungs. The study will investigate loading a model drug (MTX) onto polyamide-disulfide polymer to see if it can be used to treat asthma.

■ EXPERIMENTAL SECTION

Materials

In the present study, the chemical materials were used, including MTX from Sigma, polyamide-disulfide provided by Dr. Dalia [21], buffer phosphate saline (PBS) solution and sodium hydroxide (NaOH) is purchased from Chem Co, England, and ferric chloride ($FeCl_3$) with 98% purity purchased from Hangzhou Soya-Med (China).

Instrumentation

The spectra of Fourier-transform infrared spectroscopy were collected within 400 and 4000 cm^{-1} on a Perkin Elmer with 4 cm^{-1} resolutions and can be used as supporting data [20-22]. Four samples were analyzed the drug, polymer, polymer nanoparticles, and polymer-drug nanocomposite. A small amount of powder sample (0.01 mg) was employed, and the powder was subjected to a force gauge of roughly 70.

Ultraviolet-visible spectrophotometry is a common method used widely to qualitatively analyze. To quantitatively measure the drug release, a Shimadzu UV-1601 spectrophotometer at Isra University was used. The particle size and zeta potential of the drug-polymer nanocomposites were evaluated. Dynamic light scattering was performed with a zeta sizer (Malvern, UK) at Hikma Pharmaceutical Manufacturing. Scanning electron microscopy (FE-SEM) was used using a Zeiss LEO 1550 (Jena, Germany) instrument. The zeta sizer range can measure particle size distributions ranging from less than a nanometer up to several microns.

Procedure

Synthesis of nano polymer using $FeCl_3$ as a cross-linker

Polymer solutions were prepared by dissolving 0.05 and 0.01 g in 20 mL 0.1 M NaOH. The $FeCl_3$ as cross-linker solutions were prepared by dissolving 0.05 and 0.10 g in 25 mL water. The PNPs were prepared by placing a solution of polymer into a 250 mL beaker. After that, the cross-linker $FeCl_3$ was added dropwise to

the polymer solution. The pH was adjusted at 6.7 and 11.3 using NaOH. The PNPs were stirred overnight, separated using ultracentrifugation (11,000 rpm), washed with distilled water, and dried in the oven at 30 °C [21].

Synthesis of MTX-polymeric nanocomposites

Different amounts of MTX (0.025 and 0.050 g) were dissolved in 20 mL 0.1 M NaOH. Synthesis of MTX-polymer nanocomposite was carried out by mixing the solution of MTX (0.025 and 0.050 g) with the solution of polymer (0.050 and 0.010 g), followed by adding $FeCl_3$ solution (0.050 and 0.100 g) drop by drop into the mixture of MTX and polymer with a stirrer. The pH of the solution was controlled. The stirring was maintained for 16 h. Following that, the final products were centrifuged at 11,000 rpm and room temperature (25 °C) for 25 min to allow separation of the nanoparticles. The final product was dried in an oven to obtain the final dry powder [21,23-24].

Design of the experiment

The statistical program Minitab 18.1 was used to investigate the effects of independent variables (such as MTX, polymer, $FeCl_3$ concentration, and pH) on the percent loading efficiency and particle size by using the Placket-Burman experimental design [25]. Two levels of these variables are summarized in Table 1. Table 2 summarizes the twenty experimental trials, including the four independent variables at higher and lower levels. The effects of the variables on the response were also determined using the response surface methodology. Surface plots, main effect graphical contour plots, and interaction plots were employed in the graphical analysis.

Determination of loading efficiency for methotrexate in nanocomposite

Centrifugation was utilized to calculate the loading efficiency (LE) of MTX from produced nanocomposites. We put nanocomposites on centrifugation and then take supernatant to calculate the MTX loading efficiency. The procedure started by centrifuging the samples for 25 min at 11,000 rpm. The absorbance was taken at 370 nm for free dug-in supernatant. The equation was used to calculate LE of MTX (Eq. (1)) [26].

$$\%\ \text{loading efficiency} = \frac{\text{Total amount of MTX-free MTX drug in supernatant}}{\text{Mass of nanocomposite}} \times 100 \quad (1)$$

Aerodynamic particle size analysis using next generation impactor (NGI)

After preparing MTX nanocomposite, 0.11 g from the dried particles were milled using mortar and pestle, then the final product was manually filled into gelatin capsules with a hard shell, size 3, to be analyzed by the new generation impactor (NGI).

Table 1. Placket-Burman design levels for polymer, drug, $FeCl_3$, and pH

Levels	Polymer (g)	Drug (g)	$FeCl_3$ (g)	pH
Higher-level	0.100	0.050	0.100	11.3
Lower level	0.050	0.025	0.050	6.7

Table 2. Samples designed of polymer, drug, $FeCl_3$, and pH by Plackett-Burman design

Run order	Polymer (g)	Drug (g)	$FeCl_3$ (g)	PH	Run order	Polymer (g)	Drug (g)	$FeCl_3$ (g)	pH
1	0.050	0.050	0.050	11.3	11	0.100	0.025	0.100	6.7
2	0.100	0.025	0.050	6.7	12	0.050	0.025	0.100	11.3
3	0.100	0.025	0.050	6.7	13	0.050	0.050	0.050	6.7
4	0.100	0.050	0.100	11.3	14	0.050	0.025	0.100	6.7
5	0.050	0.025	0.050	11.3	15	0.100	0.050	0.050	11.3
6	0.100	0.050	0.100	6.7	16	0.050	0.050	0.100	11.3
7	0.100	0.025	0.100	11.3	17	0.050	0.025	0.050	11.3
8	0.050	0.025	0.100	6.7	18	0.050	0.050	0.100	6.7
9	0.100	0.025	0.050	11.3	19	0.100	0.050	0.050	6.7
10	0.100	0.050	0.100	11.3	20	0.050	0.050	0.050	6.7

To analyze the *in vitro* deposition and aerodynamic particle size distribution, NGI was used with a flow rate of 60 L/min and a flow rate of 4 s to produce 4 L. The aerosolization performance of MTX nanocomposite was determined using a capsule manually filled with 0.11 g (± 10%) of the blended drug. In the test, six capsules were used.

In each stage, samples were obtained by dissolving the contents of each tray in a 10 mL PBS. The samples were then transferred to volumetric flasks and well-filtered. UV-vis spectrometry was used to ensure stability. Samples were stored at room temperature and covered by aluminum foil to direct light.

Fine particle fraction (FPF) and emitted dose (ED) were determined for MTX-nanocomposite analysis, FPF was defined as the mass of particles by weighting each tray before and after performing the NGI test, the summation of tries from 2–7 in µg was calculated then divided it per 6 doses. The emitted dose was calculated based on the cumulative content obtained from the induction tube, pre-separator, and trays 1 to 8, based on Eq. (2) [27].

$$\text{Emitted dose} = \frac{\text{Cummulative content}}{\text{Theoretical drug content in sample}} \quad (2)$$

The release of MTX from nanocomposites in vitro

A total of 10 mg of the formulation was used to detect the release performance by placing it to 2 mL of PBS pH 7.4, using a Perkin Elmer UV-vis spectrophotometer, 370 nm was chosen as the wavelength. In addition, the device was programmed to take a reading every 10 min for 24 h. At specified time intervals, the cumulative amount of medication released into the solution was measured at the corresponding λ_{max}. The percentage release of methotrexate in the PBS was obtained in Eq. (3) [24].

$$\% \text{ release} = \frac{\text{Concentration of MTX at time (ppm)}}{\text{Concentration of MTX in the nanocomposites (ppm)}} \times 100 \quad (3)$$

Initial screening studies

Initial screening studies were carried out to develop MTX-containing polyamide disulfide nanoparticles for delivery in a DPI to the lower parts of the lung. The key success elements in the screening studies are to ensure that the produced nanoparticles meet the compendia requirements in terms of content uniformity. Further, a successful DPI should demonstrate favorable characteristics. First, the high level of the emitted dose represents the total amount of API that is discharged from the capsule and is deposited into the respiratory system, which is calculated from the amount collected in the induction tube, pre-separator, and trays 1–8 of the NGI.

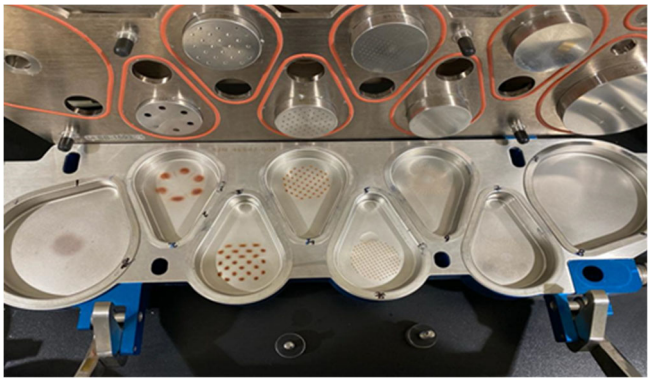

Fig 1. The dark brown powder collected from trays 1–8, which represents the MTX loaded on polyamide disulfide, is highlighted in the deposition of the nano aggregates onto the NGI apparatus

Second, the emitted dose has a high FPF, which is determined from the total amount of API collected from trays 2–7 in the NGI, which represents particles between 1–5 µm. Thirdly, the high FPF of the theoretical dose is calculated from the FPF divided by the theoretical dose of MTX. A drug particle size range of 1–5 µm is required for drug particles to reach the deep lung by inhalation, while a particle size range of 1–2.8 µm is the best for reaching the tiny airways and alveoli region [28]. Several formulations were developed, and initial results demonstrated effective deposition of the Nano capsulated onto the NGI trays as depicted in Fig. 1.

■ RESULTS AND DISCUSSION

In this work, the Minitab 18.1 software was used to evaluate the effect of different variables (concentration of polymers, drug, $FeCl_3$, and pH) on the loading efficiency and particle size as responses. Table 3 shows the Plackett-Burman design matrix. As many as 20 samples were prepared in the laboratory. Results of these samples were analyzed by Pareto charts, the normal plot

Table 3. Data outcomes of %LE and particle size for MTX-nanocomposites

Run order	Polymer (g)	Drug (g)	$FeCl_3$ (g)	pH	% LE	Size (nm)
1	0.050	0.050	0.050	11.3	48	*
2	0.100	0.025	0.050	6.7	62	152
3	0.100	0.025	0.050	6.7	59	145
4	0.100	0.050	0.100	11.3	18	295
5	0.050	0.025	0.050	11.3	41	300
6	0.100	0.050	0.100	6.7	26	360
7	0.100	0.025	0.100	11.3	20	250
8	0.050	0.025	0.100	6.7	32	160
9	0.100	0.025	0.050	11.3	57	180
10	0.100	0.050	0.100	11.3	20	275
11	0.100	0.025	0.100	6.7	33	*
12	0.050	0.025	0.100	11.3	13	*
13	0.050	0.050	0.050	6.7	55	123
14	0.050	0.025	0.100	6.7	38	150
15	0.100	0.050	0.050	11.3	*	295
16	0.050	0.050	0.100	11.3	*	240
17	0.050	0.025	0.050	11.3	44	311
18	0.050	0.050	0.100	6.7	*	120
19	0.100	0.050	0.050	6.7	*	*
20	0.050	0.050	0.050	6.7	58	130

NOTE: The symbol "*" indicates the samples deleted through the software suggestion for the increase of the R^2 value

of the standardized effects, a residual plot which includes a histogram, residual versus fits the plot, residuals versus order of the model, contour plot, main effects plot, and interaction plots.

Influence of Formulation Factors on %LE and Particle Size

ANOVA values for loading efficiency versus different factors

The analysis of variance (ANOVA) data for the loading efficiency model is shown in Table 4**.** Linear contains polymer, drug, $FeCl_3$, and pH, as shown in the table. Polymer*drug, Polymer*$FeCl_3$, Polymer*pH, Drug*pH, and lastly, $FeCl_3$*pH are all included in the 2-way interaction. By ANOVA, we can estimate if the difference between groups of factors is statistically significant or not and this depends on determining the P-value and F-value. Examining the P-value and F-value is key to determining the statistical significance. If the P values were less than 0.05, and the F values were high, which implies statistical importance. P-value is the probability of obtaining results close to those observed in the experiment, assuming that the null hypothesis is true. P-value < 0.05 indicates high evidence against the null hypothesis, which means less than 5% probability the null is correct (statistically significant). Based on the P-value using model linear and 2-way interaction.

We note from Table 4, which shows the ANOVA data for the loading efficiency model. The linear has a statistically significant effect because the P-value is less than 0.05 with the F-value of 89.52. The polymer and drug have no statistically significant effect because the value of the P-value is greater than 0.05, but the pH and $FeCl_3$ have statistically significant effects because the P-value < 0.05. Alternatively, 2-way interactions (Polymer*drug, Polymer*$FeCl_3$, and Drug*pH) do not have a statistically significant effect because the P-value is greater than 0.05, but Polymer*pH and $FeCl_3$*pH have a statistically significant effect because the P-value is less than 0.05.

Table 4. ANOVA statistical analysis of loading efficiency (%LE) and particle size

Loading efficiency model							
Source	DF	Adj SS	Adj MS	F-Value	P-Value	T-value	VIF
Model	9	4040.21	448.91	79.72	0.000		
Linear	4	2016.36	504.09	89.52	0.000		
Polymer	1	16.67	16.67	2.96	0.136	1.72	1.50
Drug	1	0.37	0.37	0.06	0.807	-0.25	2.21
$FeCl_3$	1	1555.88	1555.88	276.31	0.000	-16.62	2.13
pH	1	320.38	320.38	56.90	0.000	-7.54	1.34
2-Way interaction	5	200.10	40.02	7.11	0.017		
Polymer*Drug	1	23.06	23.06	4.10	0.089	-2.02	2.21
Polymer*$FeCl_3$	1	20.37	20.37	3.62	0.106	-1.90	2.21
Polymer*pH	1	71.50	71.50	12.70	0.012	3.56	1.34
Drug* $FeCl_3$	-	-	-	-	-	-	-
Drug*pH	1	20.30	20.30	3.61	0.106	1.90	1.34
$FeCl_3$*pH	1	56.70	56.70	10.07	0.019	-3.17	1.34
Lack of Fit	1	0.29	0.29	0.04	0.845		
R^2 value	R^2 = 99.17% R^2 (adj) = 97.93% R^2 (pred) = 96.46%						
Regression equation	%LE = 86.8 + 85 Polymer - 7 Drug - 26 $FeCl_3$ - 4.30 pH - 5600 Polymer*Drug- 2771 - Polymer*$FeCl_3$ + 42.5 Polymer*pH + 45.3 Drug*pH -37.9$FeCl_3$*pH						
Particle size model							
Source	DF	Adj SS	Adj MS	F-value	P-value	T-value	VIF
Model	9	97281.8	10809.1	180.18	0.000		
Linear	4	32596.1	8149.0	135.84	0.000		
Polymer	1	9621.8	9621.8	160.39	0.000	12.66	1.34
Drug	1	4896.7	4896.7	81.62	0.000	9.03	1.34
$FeCl_3$	1	3104.6	3104.6	51.75	0.000	7.19	1.34
pH	1	16916.2	16916.2	281.98	0.000	16.79	1.34
2-Way interaction	5	49450.3	9890.1	164.86	0.000		
Polymer*Drug	1	20475.0	20475.0	341.30	0.000	18.47	1.50
Polymer*$FeCl_3$	1	8.0	8.0	0.13	0.727	-0.37	2.13
Polymer*pH	1	16013.9	16013.9	266.94	0.000	-16.34	2.21
Drug* $FeCl_3$	1	2763.9	2763.9	46.07	0.001	-6.79	2.21
Drug*pH	1	5275.1	5275.1	87.93	0.000	-9.38	2.13
$FeCl_3$*pH	-	-	-	-	-	-	-
Lack of Fit	1	0.4	0.4	0.01	0.940		
R^2 value	R^2 = 99.63% R^2 (adj) = 99.08% R^2 (pred) = 98.54%						
Regression equation	Particle Size = -783.9 + 3604 Polymer + 4233 Drug + 3190 $FeCl_3$ + 114.24 pH + 140200 Polymer*Drug – 1650 Polymer*$FeCl_3$ - 844.7 Polymer*pH – 64571 Drug*$FeCl_3$ - 920.7 Drug*pH						

When predictors are correlated, the variance inflation factor (VIF) approach for measuring multicollinearity is used, which measures how often the variance of an assumed regression coefficient increases. When no variables are associated, the VIF must be close or equal to one, indicating that there is no multicollinearity. Because of the significant multicollinearity, the regression coefficients are badly estimated if VIF is more than 5. Table 4 shows the value of VIF for all variables less than 5, indicating that there is no multicollinearity.

The F-value is a parameter used in ANOVA analysis for comparing two variances and deciding if

these have a significant effect or not. So, if the P-value is small ($P < 0.05$) it will be significant compared to the F-value, which will be large. When the F-value is larger, the linked P-value is lower. Table 4 shows that all the F-values of the one-way and two-way interactions were larger than the P-values, indicating statistical significance, except for the drug, which has an F-value smaller than the P-value, indicating insignificance.

The T-value measures the size of the difference relative to the variation in your sample data. The relationships between the P-values and T-values were less than or equal to 0.05 with greater T-values, implying statistical significance. If the T-value is closer to zero, the more likely there is not a considerable difference. From Table 4**,** the higher T-value for Polymer*pH indicates the highest positive significant effect, while the pH has the lowest negative effect.

The degrees of freedom (DF) are the number of independent values provided by data that can be spent to select the values of unknown factors. Adjusted sum of squares (Adj SS) and adjusted mean squares (Adj MS) were included in the analysis. As seen in Table 4, there is a lack of fitness because the purpose is to ensure that the models are acceptable. Lack of fit should be non-significant at $P > 0.05$ to have the best model. The lack of fit P-value was 0.845. This implies that it is unimportant. As a result, the model is fitted.

The R-square (R^2) informs us how well the regression line predicts real values by measuring how well each data point fits the regression line. Range of R^2 from 0–100%, if the R^2 is close to 100%, has the predicted value and the actual value close together. In contrast, a low value of R^2 tells us the regression line does not fit the data that well. There are many limitations of R^2; it only takes care of the level of a correlation, does not consider the number of samples, and when independent variables are added to the model, the R^2 increases, which is misleading because some of the additional variables may be meaningless with minor significance. To overcome these problems could use the adjusted R^2 (adj.). If the useless predictors are added to the model, adjusted R^2 will decrease and vice versa. To select if the model fits the original data or not, predicted R^2 (pred.) was used. It shows how well a regression model predicts new observations' responses. The R-square value is 99.17%, the adjusted R-square is 97.93%, and the prediction R-squared is 96.46%. This indicates that the model of loading efficiency is explained for about 96.46% of the new data, which gives the ability of the model to predict a set of new data which is more logically valid.

ANOVA values for particle size versus different factors

Table 4 shows the ANOVA data for the particle size model. Linear contains Polymer, Drug, $FeCl_3$, and pH, as shown in the table. Polymer*drug, polymer*$FeCl_3$, polymer*pH, drug*$FeCl_3$, and lastly drug*pH are all included in the 2-way interaction. As mentioned above, if P-value < 0.05, the model will be statistically significant and not statistically significant if the P-value > 0.05. Based on the P-value using model linear and 2-way interaction as observed in Table 4, the linear includes polymer, drug, $FeCl_3$, and pH. All these factors have P-value < 0.05, which means these factors have significant statically. In 2-way interaction, there are many factors polymer*drug, polymer*$FeCl_3$, polymer*pH, drug*$FeCl_3$ and drug*pH. All factors except polymer*$FeCl_3$ have P-value < 0.05 which means these factors are significant statically. P-value > 0.05 means lack of fit was insignificant-value of lack of fit of particle size was 0.94, indicating that the model was the best.

The higher T-value for polymer*drug indicates the highest positive significant effect, while the polymer*pH has the lowest negative effect. The value of VIF for all variables is less than 5, and this indicates that there is no multicollinearity. From Table 4, the R^2 value of particle size is 99.63%. After modification, the adjusted R^2 value of particle size was 99.08%, and the value of the predicted R^2 was 98.54%. Because there was no statistical difference between the R^2 value and the adjusted R^2 value, the model has statistical significance.

Analysis of ANOVA Data

Pareto charts effect for %LE and particle size

The Pareto chart illustrates the standardized effects absolute value and arranges it from highest to lowest effects in columns. The Pareto chart has a reference line;

this line can indicate if this factor has a significant effect or not. If the column crosses this line, it has a significant effect and vice versa. The effect of several factors on % LE can be illustrated using the Pareto chart, as shown in Fig. 2(a). The reference line is 2.45 as four columns cross this line, and they are $FeCl_3$, pH, polymer*pH, and $FeCl_3$*pH. This means all these factors have a significant effect on %LE, and the most important one is $FeCl_3$.

It can see from the Pareto chart in Fig. 2(b), the effects of nine factors on particle size. A threshold is 2.45, so variables with standardized effects above 2.45 are significant, and others are insignificant. All factors of data cross the reference line except one factor. So, we can conclude that polymer*drug, pH, polymer*pH, polymer, drug*pH, drug, $FeCl_3$, and drug*$FeCl_3$ have a significant effect on particle size, but polymer*$FeCl_3$ is statistically insignificant. When comparing these factors to each other, there are three factors, polymer*drug, pH, and polymer*pH have the most significant effect on particle size.

Normal plot of the standardized effects

A normal plot is a tool for distinguishing active effects from those that are inert. These plots have a straight line. If any effect passes far off this line, it is declared significantly. The factors that have insignificant effects are expected to be normally distributed with a mean equal to zero. So, these effects will aggregate on along a straight line or close to it. We can conclude from Fig. 3(a) that the polymer*pH has a largely significant effect on %LE. In addition, Fig. 3(b) explains that polymer*drug, pH, polymer, drug, and $FeCl_3$ have a significant effect on size with different percentages of 92, 80, 65, 60, and 45% respectively.

Residual histogram plots for %LE and particle size

To see if the variance is normally distributed, the residual histogram was used. A bell-shaped pattern distributed around zero indicates the normal distribution of data. Fig. 4(a) and 4(b) show the residual histogram plot of %LE and particle size, respectively. From the figure, we show a bell-shaped distribution around zero, indicating normal distribution patterns.

Contour plot of loading efficiency and particle size

Analysis of data and searching for minimum and maximum effects in a set of trivariate data is one of the most advantages of a contour plot because it can arrange factors and explain their effect on each other in topographical maps shown in two-dimensional data. The horizontal axis shows one variable, and the second variable is shown on the vertical axis, the color gradient in the graph shows the third variable (124). These figures, which are shown below, explain the relationship between many of the factors: drug, polymer, pH, and $FeCl_3$ on the X and Y-axis and how both contribute to %LE and particle size.

Fig. 5(a) shows the highest %LE corresponds to a high polymer amount of 0.095 g and the concentration of the drug below 0.03 g at fixed values of $FeCl_3$ (0.075 g) and pH = 9. On the other hand, Fig. 5(b) explains the relationship between the concentration of the drug and pH. The result shows the %LE > 450 appears when the

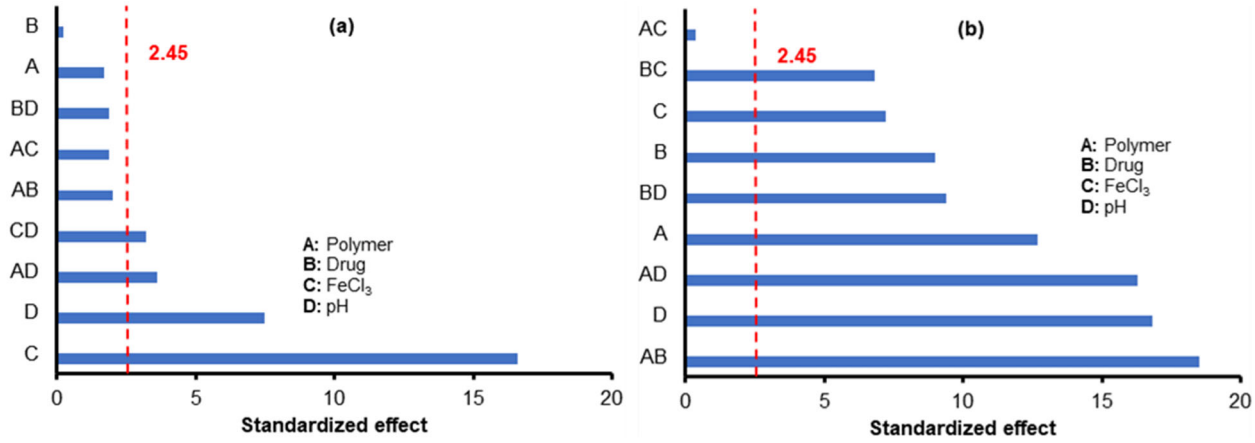

Fig 2. Pareto chart of standardized effects on (a) loading efficiency and (b) particle size

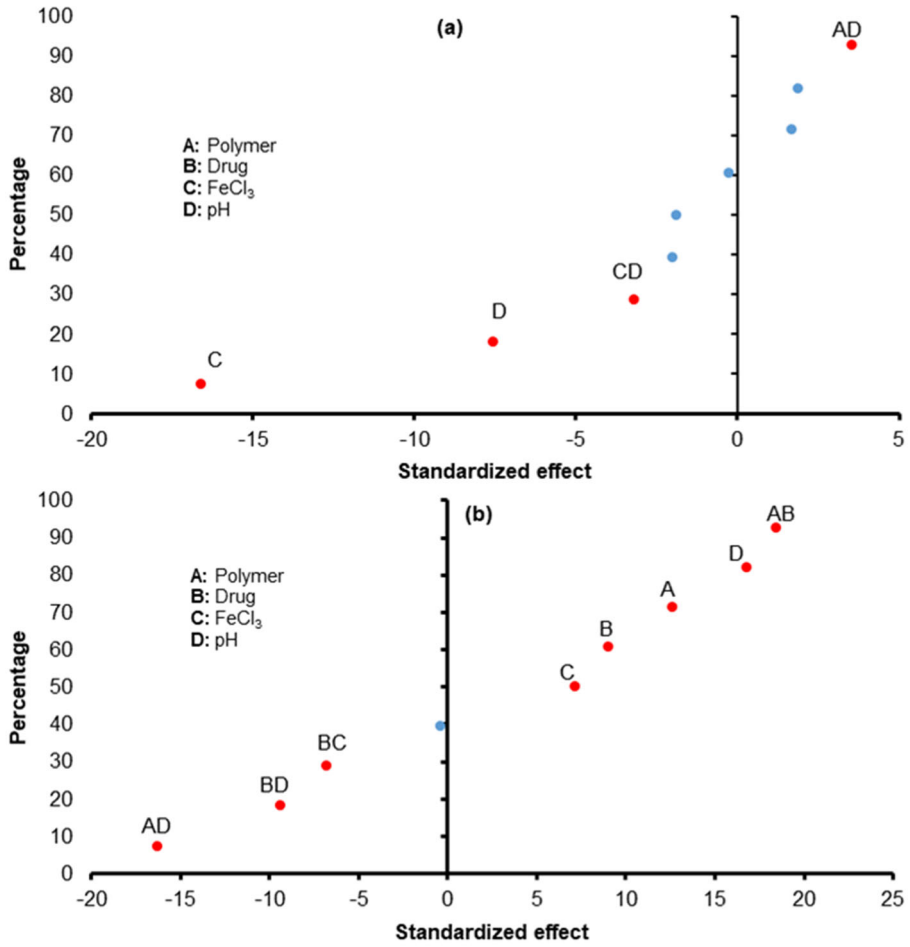

Fig 3. Normal plot of for (a) loading efficiency and (b) particle size

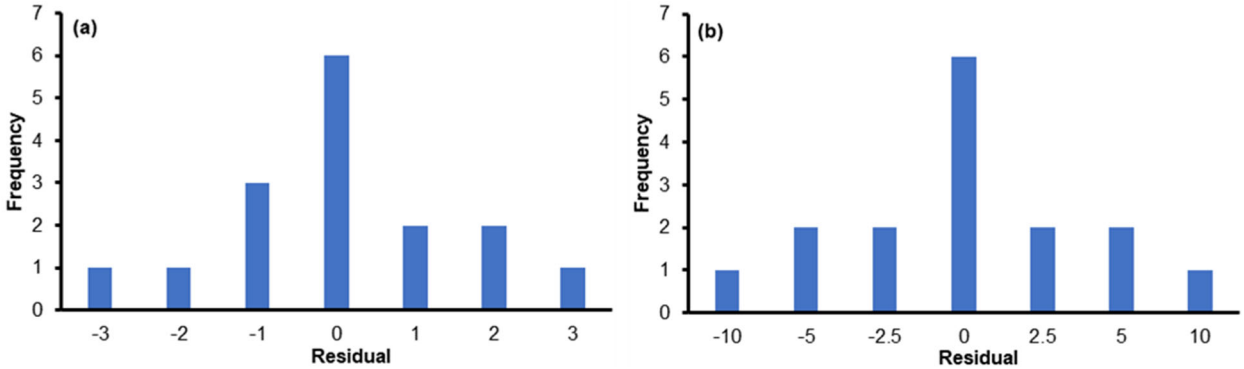

Fig 4. Histogram of model for (a) %LE and (b) particle size

concentration of drug < 0.035g and pH < 7, at fixed values of polymer 0.075 g and $FeCl_3$ 0.075 g.

Depending on Fig. 5(c) the %LE of more than 44% was reached by using a concentration of less than 0.087 g of the polymer at pH starting of 6.5–7.5, with a fixed value of drug (0.0375 g) and $FeCl_3$ (0.075 g). Fig. 5(d) illustrates when the concentration of the drug from 0.02–0.05 g and the concentration of $FeCl_3$ below than 0.057 g at fixed values of polymer (0.075 g) and pH = 9, the %LE was reached > 50%.

Based on Fig. 5(e) shows that %LE of more than 55% was achieved when the concentration of the

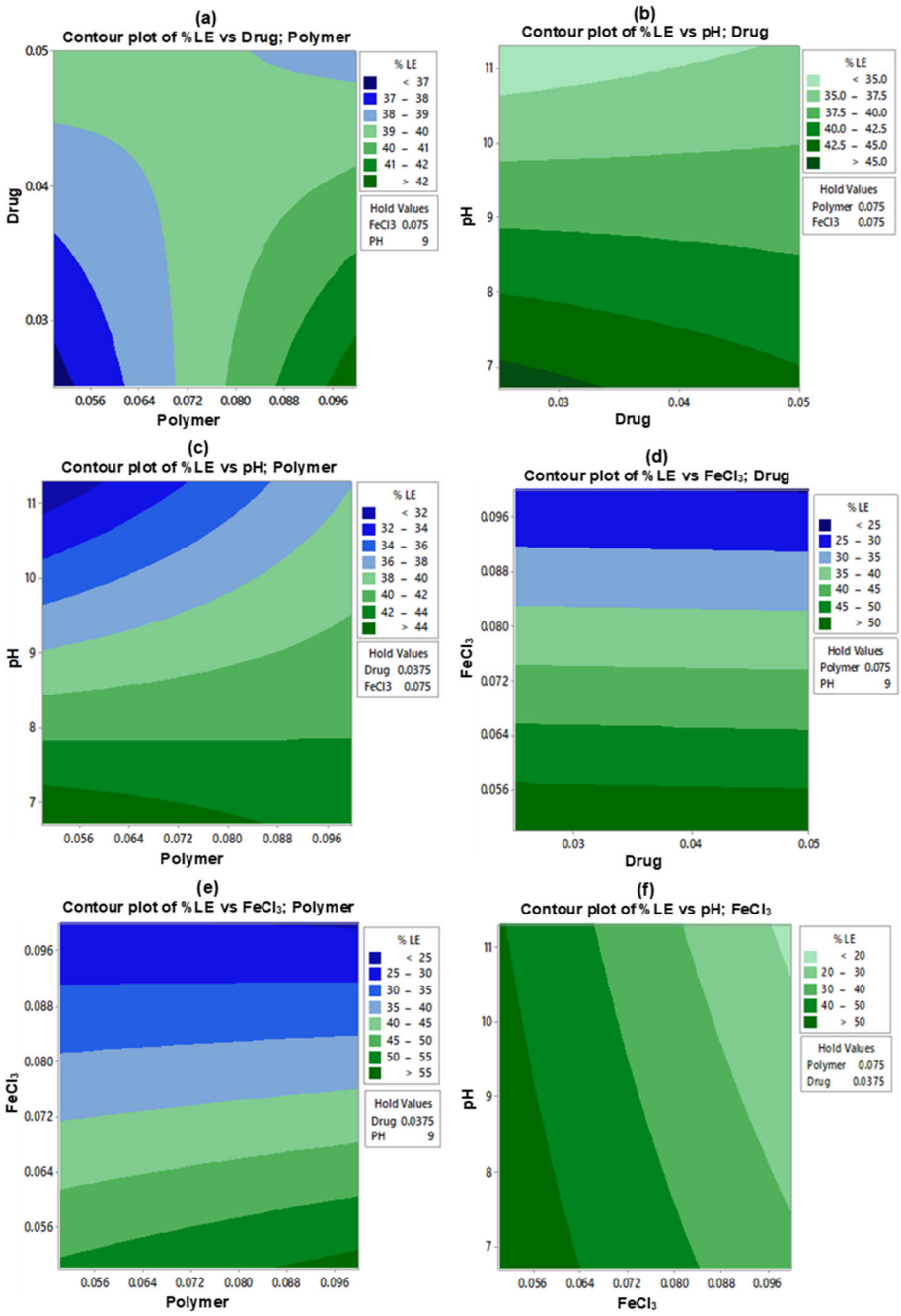

Fig 5. Contour plot of loading efficiency against pH, $FeCl_3$, polymer and drug variables

polymer was more than 0.087 g and $FeCl_3$ concentration < 0.056 g, at fixed values of the drug (0.0375 g) and pH = 9. Fig. 5(f), shown using low concertation of $FeCl_3$ <0.064 g at pH value range 6.5–11.5, with fixed values of polymer (0.075 g) and drug 0.0375 g was given the highest %LE. Fig. 6(a), shows that greater particle size was achieved when using a high level of polymer > 0.096 g and a high level of drug > 0.049 g at a fixed level of $FeCl_3$ 0.075 g and pH = 9. Fig. 6(b), shows the relationship between pH and a drug on particle size when drug concentration from 0.025–0.050 g at a high level of pH of more than 10.5 gives a greater particle size of more than 260 nm at a constant level of polymer (0.075 g) and $FeCl_3$ (0.075 g).

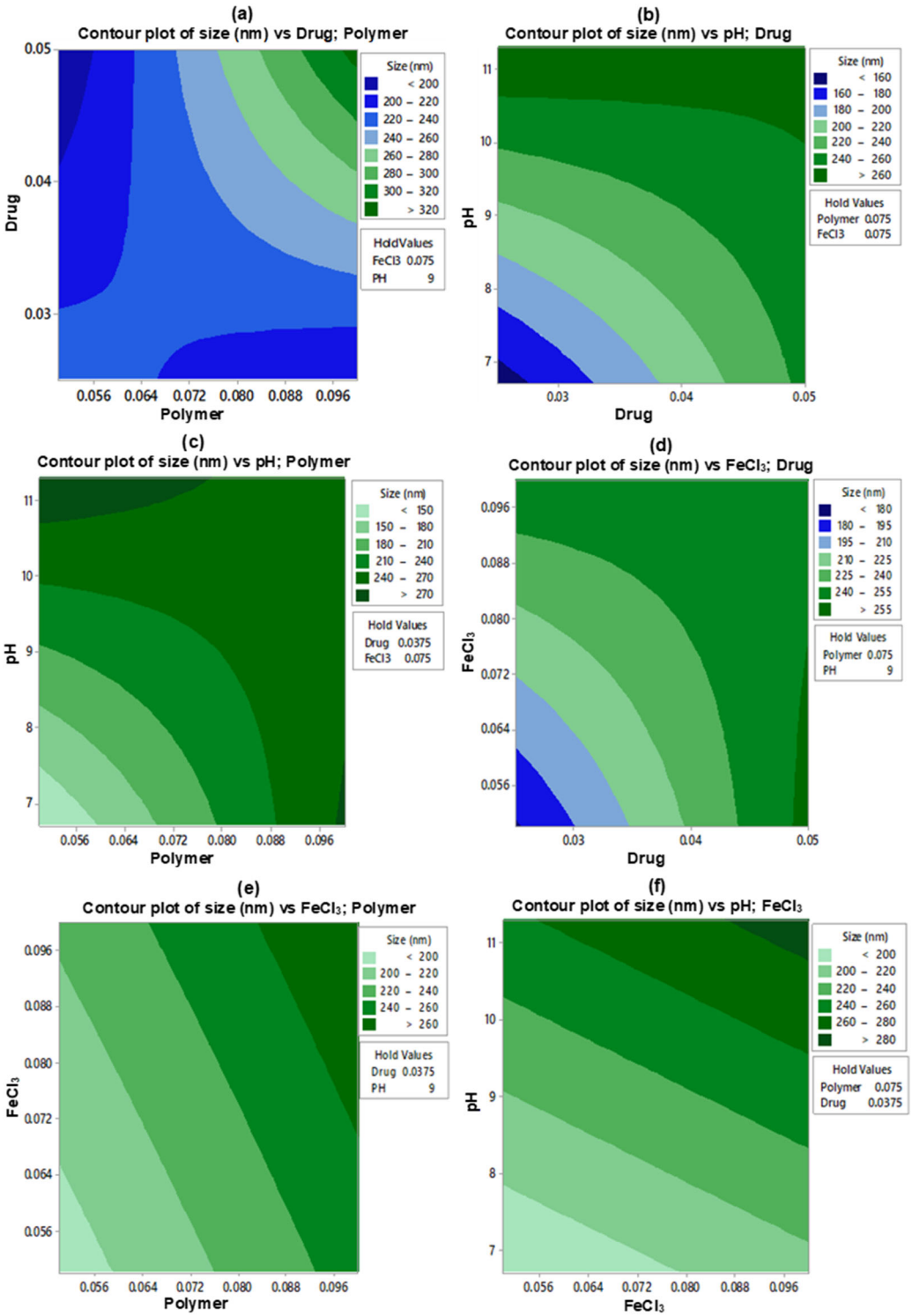

Fig 6. Contour plot of particle size against pH, $FeCl_3$, polymer and drug variables

The relationship between pH and polymer at a fixed level of the drug (0.0375 g) and $FeCl_3$ (0.075 g) is illustrated in Fig. 6(c), this figure illustrates two regions: the first one when used pH more than 10.8 with polymer concentration 0.055–0.075 g and the second when used pH less than 7 with polymer concentration above 0.096, in both, we achieved greater particle size more than 270 nm. Fig. 6(d) shows the effect of the cross-linker $FeCl_3$ and the

concentration of the drug on particle size. When used, the high level of drug > 0.048 g and $FeCl_3$ from 0.055 to 0.072 g will give a larger particle size of more than 255 nm at the constant level of polymer (0.075) g and pH = 9.

Fig. 6(e) shows how the cross-linker $FeCl_3$ and polymer affect particle size when using the level of $FeCl_3$ > 0.072 g and polymer > 0.08 g, which gives a larger particle size of more than 260 nm at a fixed level of drug (0.0375 g) and pH = 9. At the fixed level of polymer (0.075 g) and drug (0.0375 g), when studying the relationship between pH and $FeCl_3$ as shown in Fig. 6(f), the high level of pH > 10.8 and $FeCl_3$ > 0.085 g was given large particle size more than 280 nm.

Main effects plot for %LE and particle size

The main effects plot is most appropriate when we have many variables. We can then compare the changes in the level means to select which variables affect the response the most. The main effects plots give the optimal combination of testing parameters.

Fig. 7(a) shows the polymer having a slightly positive effect on loading efficiency. However, drug concentration does not have any effect on %LE. Fig. 7(a) also shows the concentration of $FeCl_3$ indirectly affected the %LE. The %LE will decrease from 60 to 20 while increasing the concentration of $FeCl_3$ from 0.0500 up to 0.1007 g. Like $FeCl_3$ the pH has negatively correlated with %LE. Fig. 7(b) illustrates the concentration of the polymer and drug has a positive correlation with particle size. The particle size will reach 260 nm, and 255 nm when the concentration of the polymer and drug is increased to 0.10 and 0.05 g respectively. Fig. 7(b) also shows a positive correlation, when the used concentration of cross-linker $FeCl_3$ from 0.05 to 0.10 g, it will increase the particle size directly. Fig. 7(b) shows the link between pH and particle size. The increased level of pH from 7 to 11 causes the particle size to start increasing from 200 to 280 nm, according to the figure.

Optimization of %LE and particle size

Fig. 8 was created using software. The red line was moved to achieve these new values for each polymer, drug, $FeCl_3$, and pH. As a result, altering the values of the previous four parameters would result in new predictions for percent LE and particle size. Experimental data for percent LE and particle size were obtained after the samples were prepared in the lab. Using the Bias equation, we can then calculate and examine the difference between the expected and experimental results.

Validation of the models

Table 5 shows the result of the comparison between predicted and experimental values, and a bias equation was used with validated variables. Bias reading

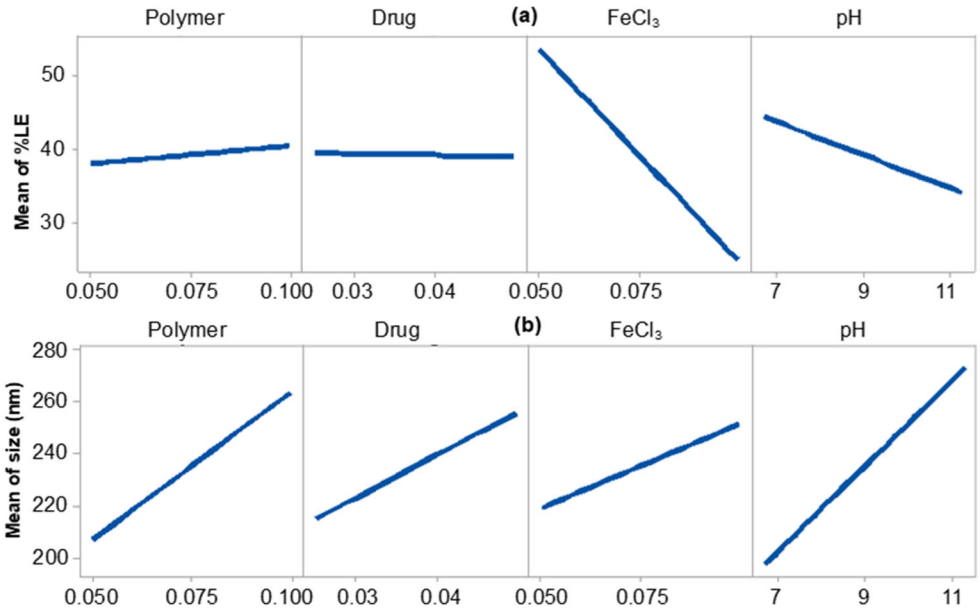

Fig 7. Main effects plot for (a) loading efficiency and (b) particle size

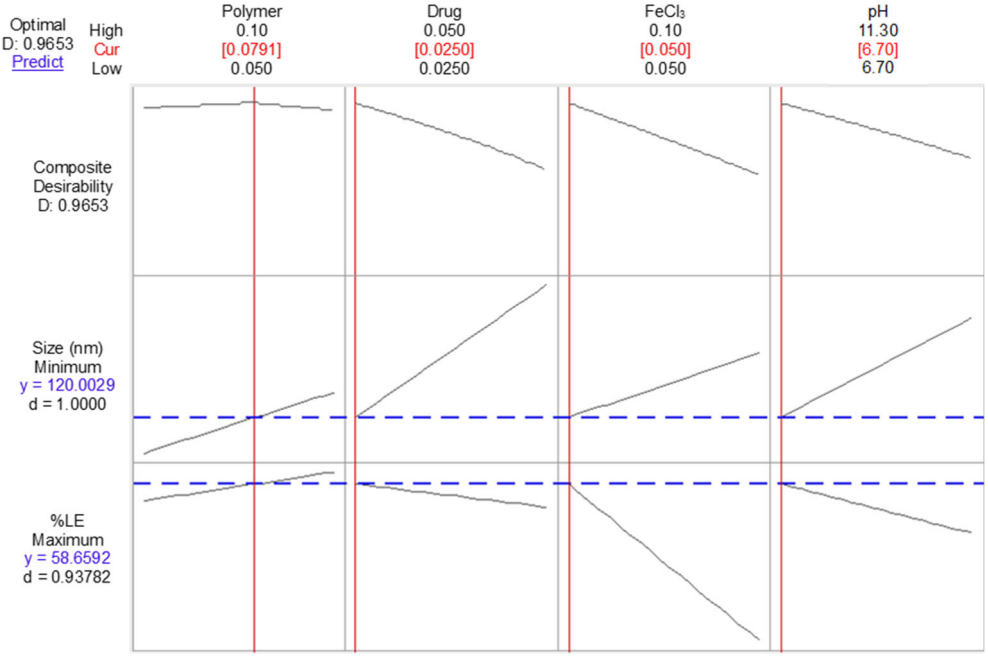

Fig 8. The optimization concentration for response factors loading efficiency and particle size

Table 5. Comparison of observed and predicted response values of optimized formulation variables

Concentrations	Experimental response	Predicted values	Observed values	Bias (%)
Polymer (79.1 mg)	LE (%)	58.7%	51.9%	−11.6%
Drug (25 mg)	Particles size (nm)	120	136	13.3%
$FeCl_3$ (50 mg)				
pH = 6.7				
Polymer (88.2 mg)	LE (%)	48.9%	45.2%	−7.6%
Drug (31.4 mg)	Particles size (nm)	206	222	7.8%
$FeCl_3$ (64.1 mg)				
pH = 7.95				
Polymer (80 mg)	LE (%)	45.8%	43.7%	−5.2%
Drug (37.7 mg)	Particles size (nm)	213	235	10.3%
$FeCl_3$ (71.4 mg)				
pH = 6.86				
(observed value – predict value / predict value) × 100 was used to determine percent bias				

was within −11.6 and 13.3% for the first sample polymer = 79.1 mg, drug = 2 5 mg, $FeCl_3$ = 50 mg, and pH = 6.7. Additionally, the values of bias were −7.6%, 7.8% for the second sample polymer = 88.2 mg, drug = 131.4 mg, $FeCl_3$ = 64.1 mg, and pH = 7.95. Regarding the third sample, polymer = 80 mg, drug = 37.7 mg, $FeCl_3$ = 71.4 and pH = 8.86, the values of bias were −5.2 and 10.3%. There is no variation between predicted and experimental values, and there is a good link in outcomes between experimental and predicted values, indicating that the models utilized in this study are accurate and valid.

Aerodynamic Performance of the MTX-Polymer Nano composition Using NGI

The MTX-polymer nanocomposite demonstrated excellent aerodynamic performance, as can be seen in Fig. 9. The Emitted dose (%ED) denotes the percentage of the nominated dose that leaves the capsule and aerosolized inhaler. This percentage presents good

aerodynamic performance of the active pharmaceutical ingredient. The key parameter is the mass transfer towards the lower parts of the respiratory system, which is presented by the respirable dose (RD), which represented almost 400 mcg per puff. This corresponds to almost 34.6% of the emitted dose (FPF-ED). The last variable is the FPF of the nominated dose. The results of the NGI analysis demonstrated that 28.1% of the nominated dose in each puff reached the lower parts of the respiratory system.

Characterization of MTX-Polymer

FTIR

Fig. 10(a-d) shows the FTIR spectra for MTX, polymer, polymer nanoparticle, and nanocomposite, respectively. The intense broad of MTX at 3450 and 3080 cm^{-1}, respectively, reflect the hydroxyl group (OH) from the carboxyl group and primary amine stretching, as illustrated in Fig. 10(a). However, bands of N–H bending from an amide group occurred in the 1550–1500 cm^{-1} range and overlapped with the aromatic C=C stretching group. Other carboxylic acid bands correlate to C–O stretching in the spectral range 1400–1200 cm^{-1}. The C=O stretching from carboxylic acid is indicated at 1600–1670 cm^{-1} [29]. Fig. 10(b) shows the polymer's FTIR spectrum. It indicated two unique infrared stretching patterns associated with the carboxyl group and the carboxyl group's hydroxyl group (OH). It found the band at 3010–3500 cm^{-1} and carbonyl group stretching vibrations at 1632 cm^{-1}. It also exhibits two peaks for the benzene group at 1406 and 1494 cm^{-1}. The stretching of the C–O bond in the carboxylic acid group is indicated by a peak at 1223 cm^{-1}. The methyl group of alkanes also causes C–H stretching at 2988 cm^{-1} [30].

Fig. 10(c) displays the characters FTIR peak for polymer nanoparticles, which are formed by the interaction of Fe^{3+} with the negatively charge of the polymer. From the figure, some of the bands disappear due to the interaction. The peak at 1600 cm^{-1} was due to the carbonyl group. Fig. 10(d) shows the FTIR peaks of MTX-polymer nanocomposite.

Scanning electron microscopy (SEM)

Fig. 11(a-b) shows the SEM image of the sample MTX-polymer nanocomposites with two magnifications 250.00 and 100.00 KX, respectively. It is clear from the image that uniformly distributed, high cluster and heterogeneous particles.

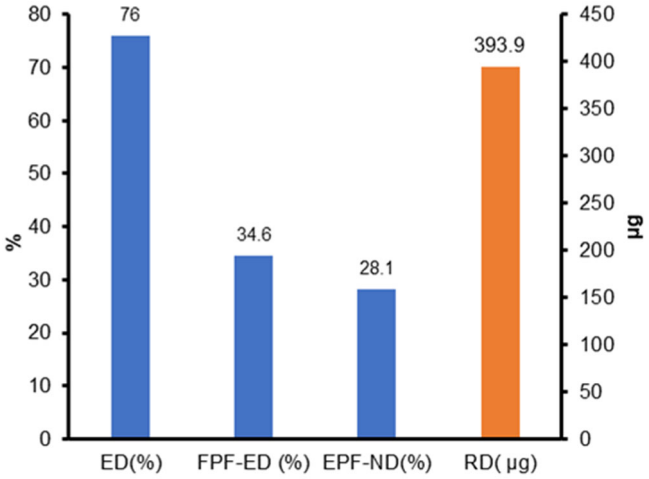

Fig 9. Aerodynamic performance of the MTX-loaded nanoparticles using NGI

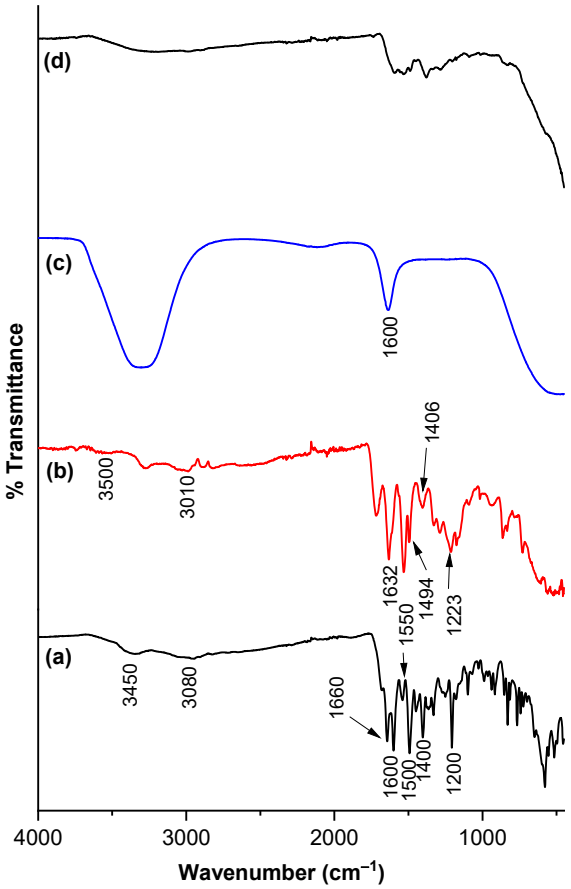

Fig 10. FTIR spectrum of (a) MTX, (b) polymer, (c) Polymer nanoparticle, and (d) MTX – nanocomposites

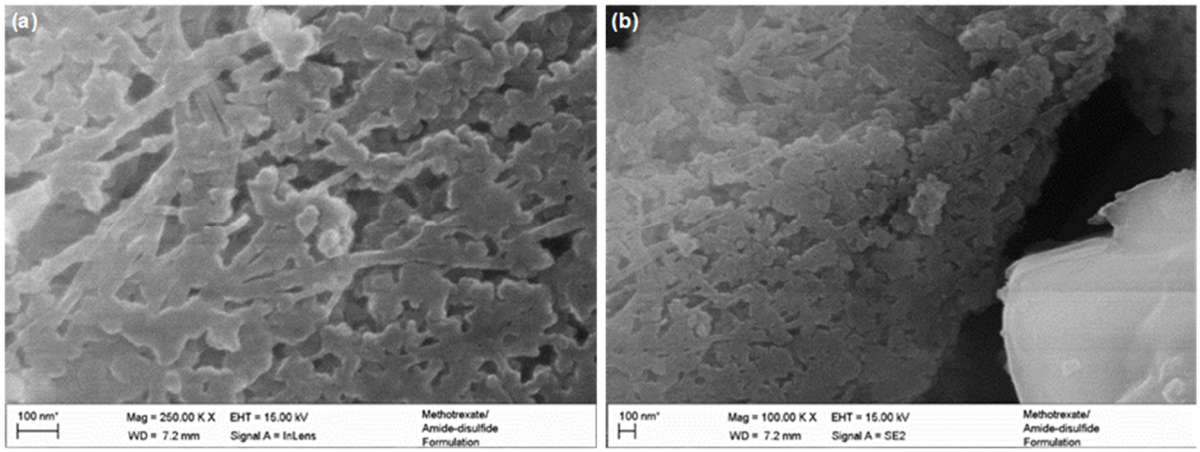

Fig 11. SEM image of MTX-polymer nanocomposites with (a) 250.00 and (b) 100.00 KX

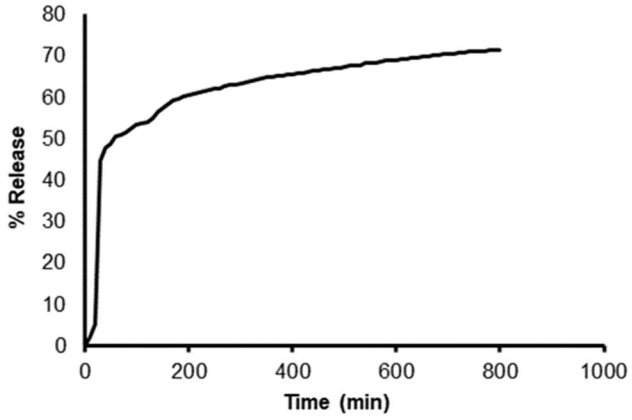

Fig 12. *In vitro* release of MTX-nanocomposites in PBS at pH 7.4

In vitro *release study of MTX from nanocomposites*

Using a microplate spectrophotometer (Thermo Fisher, Finland) and a wavelength of 370 nm, nanocomposites were placed in PBS pH 7.4 to determine the release performance. In addition, the device was programmed to take a reading every 10 min for 24 h. At certain time intervals, the total amount of drug released into the solution was measured at the corresponding λ_{max}. The amount of methotrexate released from nanocomposite in the samples was approximately 80%. Fig. 12 shows the release curves of MTX from the MTX-nanocomposites into PBS at a pH of 7.4. MTX release from the nanocomposites occurs in two release steps; the first release step starts from the beginning up to 60 min, followed by a continuous release phase within 60 min. Within the first 60 min, the maximum release was 50%, this is caused by the possibility of the drug on the surface. The second-stage release occurred up to 1400 min with complete releases of 30%. These results were due to the internal drug release.

■ CONCLUSION

The MTX-nanocomposite design with desirability properties to the respiratory system is effective in optimizing methotrexate loaded-polymer and in understanding the effects of the formulation factors on dependent variables. The results of the NGI analysis demonstrated that 28.1% of the nominated dose in each puff reached the lower parts of the respiratory system.

■ ACKNOWLEDGMENTS

The author would like to thank the Faculty of Pharmacy at Isra University for providing funding for this research under grand number 2021/2022/27-11.

■ CONFLICT OF INTEREST

The authors declare that they have no conflicts of interest.

■ AUTHOR CONTRIBUTIONS

Conceptualization – Aseel Khaled Mohammad AL-Sarayrah, Samer Hasan Hussein-Al-Ali; Data curation – Aseel Khaled Mohammad AL-Sarayrah, Samer Hasan Hussein-Al-Ali; Formal analysis – Aseel Khaled Mohammad AL-Sarayrah, Samer Hasan Hussein-Al-Ali; Funding acquisition – Aseel Khaled Mohammad AL-Sarayrah, Samer Hasan Hussein-Al-Ali, Mike Khalil Haddad; Investigation – Aseel Khaled

Mohammad AL-Sarayrah, Samer Hasan Hussein-Al-Ali; Methodology – Aseel Khaled Mohammad AL-Sarayrah, Samer Hasan Hussein-Al-Ali, Dalia Kalil; Project administration – Samer Hasan Hussein-Al-Ali ; Resources – Aseel Khaled Mohammad AL-Sarayrah, Samer Hasan Hussein-Al-Ali, Mike Khalil Haddad; Software – Samer Hasan Hussein-Al-Ali; Supervision – Samer Hasan Hussein-Al-Ali; Validation – Aseel Khaled Mohammad AL-Sarayrah, Samer Hasan Hussein-Al-Ali; Visualization – Aseel Khaled Mohammad AL-Sarayrah, Samer Hasan Hussein-Al-Ali, Mike Khalil Haddad; Writing – original draft – Aseel Khaled Mohammad AL-Sarayrah, Samer Hasan Hussein-Al-Ali.

■ REFERENCES

[1] Mims, J.W., 2015, Asthma: Definitions and pathophysiology, *Int. Forum Allergy Rhinol.*, 5 (S1), S2–S6.

[2] Caramori, G., Nucera, F., Mumby, S., Lo Bello, F., and Adcock, I.M., 2022, Corticosteroid resistance in asthma: Cellular and molecular mechanisms, *Mol. Aspects Med.*, 85, 100969.

[3] Pinnock, H., Epiphaniou, E., Pearce, G., Parke, H., Greenhalgh, T., Sheikh, A., Griffiths, C.J., and Taylor, S.J., 2015, Implementing supported self-management for asthma: A systematic review and suggested hierarchy of evidence of implementation studies, *BMC Med.*, 13 (1), 127.

[4] Khosa, J.K., Louie, S., Lobo Moreno, P., Abramov, D., Rogstad, D.K., Alismail, A., Matus, M.J., and Tan, L.D., 2023, Asthma care in the elderly: Practical guidance and challenges for clinical management-a framework of 5 "Ps", *J. Asthma Allergy*, 16, 33–43.

[5] Balde, A., Kim, S.K., Benjakul, S., and Nazeer, R.A., 2022, Pulmonary drug delivery applications of natural polysaccharide polymer derived nano/micro-carrier systems: A review, *Int. J. Biol. Macromol.*, 220, 1464–1479.

[6] Kumar, R., Mehta, P., Shankar, K.R., Rajora, M.A., Mishra, Y.K., Mostafavi, E., and Kaushik, A., 2015, Nanotechnology-assisted metered-dose inhalers (MDIs) for high-performance pulmonary drug delivery applications, *Pharm. Res.*, 39 (11), 2831–2855.

[7] Ibrahim, M., Verma, R., and Garcia-Contreras, L., 2015, Inhalation drug delivery devices: Technology update, *Med. Devices: Evidence Res.*, 8, 131–139.

[8] Kumar, M., Hilles, A.R., Almurisi, S.H., Bhatia, A., and Mahmood, S., 2023, Micro and nano-carriers-based pulmonary drug delivery system: Their current updates, challenges, and limitations – A review, *JCIS Open*, 12, 100095.

[9] Shakeel, F., 2023, Editorial: Nanomedicine-based drug delivery systems: Recent developments and future prospects, *Molecules,* 28 (10), 4138.

[10] Mehta, P.P., and Dhapte-Pawar, V., 2023, "Multifunctional Cyclodextrins Carriers for Pulmonary Drug Delivery: Prospects and Potential" in *Pulmonary Drug Delivery Systems: Material and Technological Advances*, Springer Nature Singapore, Singapore, 247–279.

[11] Sanchis, J., Corrigan, C., Levy, M.L., and Viejo, J.L., 2013, Inhaler devices – From theory to practice, *Respir. Med.*, 107 (4), 495–502.

[12] Siahaan, P., Mentari, N.C., Wiedyanto, U.O., Hudiyanti, D., Hildayani, S.Z., and Laksitorini, M.D., 2017, The optimum conditions of carboxymethyl chitosan synthesis on drug delivery application and its release of kinetics study, *Indones. J. Chem.,* 17 (2), 291–300.

[13] Astuti, I.Y., Marchaban, M., Martien, R., and Nugroho, A.E., 2017, Design and optimization of self nano-emulsifying drug delivery system containing a new anti-inflammatory agent pentagamavunon-0, *Indones. J. Chem.*, 17 (3), 365–375.

[14] Lestari, D., Nizardo, N.M., and Mulia, K., 2022, Enhanced drug release of poly (lactic-co-glycolic acid) nanoparticles modified with hydrophilic polymers: Chitosan and carboxymethyl chitosan, *Indones. J. Chem.*, 22 (5), 1338–1347.

[15] Friedman, B., and Cronstein, B., 2019, Methotrexate mechanism in treatment of rheumatoid arthritis, *Jt., Bone, Spine,* 86 (3), 301–307.

[16] Sharma, M., and Chauhan, P.M.S., 2012, Dihydrofolate reductase as a therapeutic target for

infectious diseases: Opportunities and challenges, *Future Med. Chem.*, 4 (10), 1335–1365.

[17] Nalwa, H.S., Prasad, P., Ganguly, N.K., Chaturvedi, V., and Mittal, S.A., 2023, Methotrexate intolerance in rheumatoid arthritis, *Transl. Med. Commun.*, 8 (1), 10.

[18] Gürler, M., Selcuk, E.B., Özerol, B.G., Tanbek, K., Taşlıdere, E., Yıldız, A., Yağın, F.H., and Gürel, E., 2023, Protective effect of dexpanthenol against methotrexate-induced liver oxidative toxicity in rats, *Drug Chem. Toxicol.*, 46 (4), 708–716.

[19] Sandhu, J., Kumar, A., and Gupta, S.K., 2022, The therapeutic role of methotrexate in chronic urticaria: A systematic review, *Indian J. Dermatol. Venereol. Leprol.*, 88 (3), 313–321.

[20] Song, G.G., and Lee, Y.H., 2021, Methotrexate for treating polymyalgia rheumatica: A meta-analysis of randomized controlled trials, *Int. J. Clin. Pharmacol. Ther.*, 59 (5), 366–371.

[21] Alkurdi, N.M., Hussein-Al-Ali, S.H., Albalwi, A., Haddad, M.K., Aldalahmed, Y., and Ali, D.K., 2022, Development and evaluation of a novel polymer drug delivery system using cromolyn-polyamides-disulfide using response surface design, *J. Chem.*, 2022, 7903310.

[22] Kourkoumelis, N., Zhang, X., Lin, Z., and Wang, J., 2019, Fourier transform infrared spectroscopy of bone tissue: Bone quality assessment in preclinical and clinical applications of osteoporosis and fragility fracture, *Clin. Rev. Bone Miner. Metab.*, 17 (1), 24–39.

[23] Almahamid, Y.R., Hussein-Al-Ali, S.H., and Haddad, M.K., 2022, Application of factorial design and response surface methodology in the optimization of clindamycin nanocomposites, *J. Nanomater.*, 2022, 1967606.

[24] Ahmed, Z.A.G., Hussein-Al-Ali, S.H., Ibrahim, I.A.A., Haddad, M.K., Ali, D.K., Hussein, A.M., and Abu Sharar, A.A., 2022, Development and evaluation of amlodipine-polymer nanocomposites using response surface methodology, *Int. J. Polym. Sci.*, 2022, 3427400.

[25] Kahled, E., Fouad, M.F., Badawi, M.H., Abd El-Rahim, W.M., Shawky, H., and Moawad, H., 2022, Thermostable protease, amylase and lipase enzymes of thermophilic bacteria isolated from Egyptian hot springs, *Egypt. J. Chem.*, 65 (10), 225–238.

[26] Hussein-Al-Ali, S.H., Kura, A., Hussein, M.Z., and Fakurazi, S., 2018, Preparation of chitosan nanoparticles as a drug delivery system for perindopril erbumine, *Polym. Compos.*, 39 (2), 544–552.

[27] Aganovic, A., Cao G., Kurnitski, J., and Wargocki, P., 2023, New dose-response model and SARS-CoV-2 quanta emission rates for calculating the long-range airborne infection risk, *Build Environ.*, 228, 109924.

[28] Labiris, N.R., and Dolovich, M.B., 2003, Pulmonary drug delivery. Part I: Physiological factors affecting therapeutic effectiveness of aerosolized medications, *Br. J. Clin. Pharmacol.*, 56 (6), 588–599.

[29] Fuliaş, A., Popoiu, C., Vlase, G., Vlase, T., Oneţiu, D., Săvoiu, G., Simu, G., Pătruţescu, C., Ilia, G., and Ledeţi, I., 2014, Thermoanalytical and spectroscopic study on methotrexate – active substance and tablet, *Dig. J. Nanomater. Biostruct.*, 9 (1), 93–98.

[30] Ali, D.K., Al-Zuheiri, A.M., and Sweileh, B.A., 2017, pH and reduction sensitive bio-based polyamides derived from renewable dicarboxylic acid monomers and cystine amino acid, *Int. J. Polym. Anal. Charact.*, 22 (4), 361–373.